Analytical study of electronic structure in armchair graphene nanoribbons

Huaixiu Zheng,[1] Z. F. Wang,[2] Tao Luo,[2] Q. W. Shi,[2,*] and Jie Chen[1,†]
[1]*Electrical and Computer Engineering, University of Alberta, Canada AB T6G 2V4*
[2]*Hefei National Laboratory for Physical Sciences at Microscale, University of Science and Technology of China, Hefei, Anhui 230026, People's Republic of China*

(Received 19 December 2006; revised manuscript received 18 March 2007; published 20 April 2007)

We present the analytical solution of the wave function and energy dispersion of armchair graphene nanoribbons (GNRs) based on the tight-binding approximation. By imposing the hard-wall boundary condition, we find that the wave vector in the confined direction is discretized. This discrete wave vector serves as the index of different subbands. Our analytical solutions of wave function and associated energy dispersion reproduce the results of numerical tight-binding and the solutions based on the $\mathbf{k}\cdot\mathbf{p}$ approximation. In addition, we also find that all armchair GNRs with edge deformation have energy gaps, which agrees with recently reported first-principles calculations.

DOI: 10.1103/PhysRevB.75.165414 PACS number(s): 73.61.Wp, 73.20.At

I. INTRODUCTION

Graphene, as a promising candidate of future nanoelectronic components, has recently attracted intensive research attention.[1–6] Graphene consists of a single atomic layer of graphite, which can also be viewed as a sheet of unrolled carbon nanotube. Several anomalous phenomena ranging from half integer quantum Hall effect, nonzero Berry's phase,[3] to minimum conductivity[2] have been observed in experiments. These unusual transport properties may lead to novel applications in carbon-based nanoelectronics. In addition, the carriers in graphene behave as massless relativistic particles with an effective "speed of light" $c_* \approx 10^6$ m/s within the low-energy range ($\varepsilon < 0.5$ eV).[3] These massless Dirac fermions in graphene manifest various quantum electrodynamics (QED) phenomena in the low-energy range such as the Klein paradox phenomenon.[6] Ribbons with a finite width of graphene, referred to as graphene nanoribbons (GNRs), have also been studied extensively.[7–14] Recent experiments by using the mechanical method[3,2] and the epitaxial growth method[4,15] show it is possible to make GNRs with various widths.

The carbon atoms on the edge of GNRs have two typical topological shapes, namely armchair and zigzag. The analytical wave function and energy dispersion of zigzag nanoribbons have been derived by several research groups.[16,17] For armchair GNRs, the analytical forms of wave functions within the low-energy range have been worked out based on the effective-mass approximation.[14] It is predicted that all zigzag GNRs are metallic with localized states on the edges,[8,9,16,17] while armchair GNRs are either metallic or insulating, depending on their widths.[7–10,14,16] To date, there is no general expression of the wave function in armchair GNRs. In this paper, we derive a general analytical expression of wave function and eigenenergy in armchair GNRs applicable to various energy ranges. In Sec. II, we focus on perfect armchair GNRs without any edge deformation and derive the energy dispersion by imposing the hard-wall boundary condition. Due to the quantum confinement, the spectrum breaks into a set of subbands and the wave vector along the confined direction becomes discretized, which is similar to the case of carbon nanotubes.[20] We observe that the electronic structure of perfect armchair GNRs strongly depends on the width of the ribbon. The system, for instance, is metallic when $n=3m+2$ and is insulating otherwise, where m is an integer.[7–10,14,16] Furthermore, we study the low-energy electronic structure. The linear dispersion relation is observed in armchair GNRs. In Sec. III, we evaluate the effect of deformations on the edges on the electronic structure of armchair GNRs. Calculation results based on the derived analytical wave function show that all armchair GNRs have nonzero energy gaps due to the variation of hopping integral near the edges. This observation is in line with the recently reported first-principle calculations.[11]

II. PERFECT ARMCHAIR GRAPHENE NANORIBBON

The structure of armchair GNRs consists two types of sublattices A and B as illustrated in Fig. 1. The unit cell contains n A-type atoms and n B-type atoms. Based on the

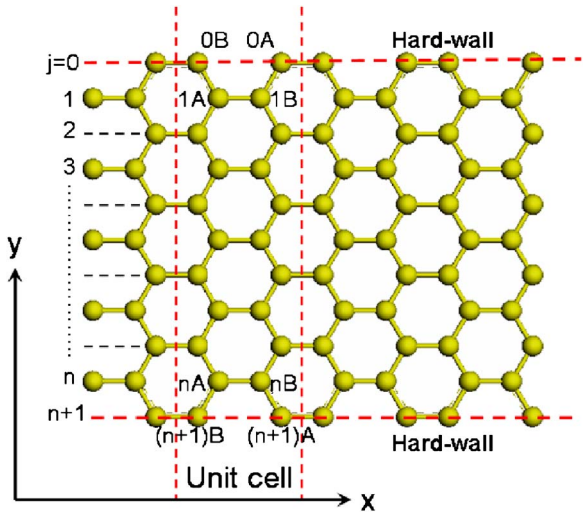

FIG. 1. (Color online) Structure of an armchair graphene nanoribbon, consisting of sublattices A and B. The width of the armchair GNR is n. Every unit cell contains n numbers of A and B sublattices. Two additional hard walls ($j=0$, $n+1$) are imposed on both edges.

translational invariance, we choose the plane-wave basis along the x direction. Within the tight-binding model, the wave functions of A and B sublattices can be written as

$$|\psi\rangle_A = \frac{1}{N_A}\sum_{i=1}^{n}\sum_{x_{A_i}} e^{ik_x x_{A_i}}\phi_A(i)|A_i\rangle,$$

$$|\psi\rangle_B = \frac{1}{N_B}\sum_{i=1}^{n}\sum_{x_{B_i}} e^{ik_x x_{B_i}}\phi_B(i)|B_i\rangle, \tag{1}$$

where $\phi_A(i)$ and $\phi_B(i)$ are the components for A and B sublattices in the y direction, which is perpendicular to the edge. $|A_i\rangle$ and $|B_i\rangle$ are the wave functions of the p_z orbit of a carbon atom located at A and B sublattices, respectively. To solve $\phi_A(i)$ and $\phi_B(i)$, we employ the hard-wall boundary condition

$$\phi_A(0) = \phi_B(0) = 0,$$

$$\phi_A(n+1) = \phi_B(n+1) = 0. \tag{2}$$

Choosing $\phi_A(i)=\phi_B(i)=\sin\left(\frac{\sqrt{3}q_y a}{2}i\right)$ and substituting them into Eq. (2), we get

$$q_y = \frac{2}{\sqrt{3}a}\frac{p\pi}{n+1}, \quad p = 1,2,\ldots,n. \tag{3}$$

q_y is the discretized wave vector in the y direction and a $=1.42$ Å is the bond length between carbon atoms. To obtain the normalized coefficients, N_A and N_B, we introduce the normalization condition

$${}_A\langle\psi|\psi\rangle_A = {}_B\langle\psi|\psi\rangle_B = 1.$$

It is straightforward to obtain $N_A=N_B=\sqrt{\frac{N_x(n+1)}{2}}$, where N_x is the number of unit cells along the x direction. The total wave function of the system can be constructed by the linear combination of ψ_A and ψ_B,

$$|\psi\rangle = C_A\left[\sqrt{\frac{2}{N_x(n+1)}}\sum_{i=1}^{n}\sum_{x_{A_i}} e^{ik_x x_{A_i}}\sin\left(\frac{\sqrt{3}q_y a}{2}i\right)|A_i\rangle\right] + C_B\left[\sqrt{\frac{2}{N_x(n+1)}}\sum_{i=1}^{n}\sum_{x_{B_i}} e^{ik_x x_{B_i}}\sin\left(\frac{\sqrt{3}q_y a}{2}i\right)|B_i\rangle\right]. \tag{4}$$

Under the tight-binding approximation, the Hamiltonian of the system is

$$H = \sum_i \varepsilon_i|i\rangle\langle i| - \sum_{\langle i,j\rangle} t_{i,j}(|i\rangle\langle j|), \tag{5}$$

where $\langle i,j\rangle$ denotes the nearest neighbors.

In perfect armchair GNRs, we set $t_{i,j}=t$ and $\varepsilon_i=\varepsilon$. By Substituting Eqs. (4) and (5) into the Schrodinger equation, we can easily obtain the following matrix expression:

$$\begin{pmatrix} \varepsilon & \mu \\ \mu^* & \varepsilon \end{pmatrix}\begin{pmatrix} C_A \\ C_B \end{pmatrix} = E\begin{pmatrix} C_A \\ C_B \end{pmatrix}, \tag{6}$$

where $\mu={}_A\langle\psi|H|\psi\rangle_B=-t\left[2e^{ik_x a/2}\cos\left(\frac{\sqrt{3}a}{2}q_y\right)+e^{-ik_x a}\right]$. Solving Eq. (6), we get the energy dispersion and wave function as

$$E = \varepsilon \pm |\mu|,$$

$$|\psi\rangle_{\pm} = \frac{\sqrt{2}}{2}\left(|\psi\rangle_A \pm \sqrt{\frac{\mu^*}{\mu}}|\psi\rangle_B\right). \tag{7}$$

Here, $\pm$ denotes the conduction and valance bands, respectively. $-\frac{\pi}{2}\leqslant\frac{3k_x a}{2}\leqslant\frac{\pi}{2}$ is required within the first Brillouin zone (BZ). These results are valid for various energy ranges.

Figure 2 shows the energy dispersion for perfect armchair GNRs with width $n=6$, 7 and 8. Here, we set $\varepsilon=0$. The results are the same as those obtained by using the numerical tight-binding method. The electronic structures of armchair GNRs depend strongly on their widths. When $n=8$, the lowest conduction band and the upmost valence band touch at the Dirac point, which leads to the metallic behavior of n $=8$ armchair GNRs. Armchair GNRs, however, are insulating when $n=6$ and $n=7$. Armchair GNRs with the width of n $=3m+2$ (m is an integer) are generally metallic and otherwise are insulating.[8,14] In addition, we observe several interesting features in the band structures of armchair GNRs.

(i) A flat conduction or valence band ($p=4$) exists, if n $=7$ as shown in Fig. 2(b). Such a flat band generally corresponds to $\frac{p}{n+1}=\frac{1}{2}$ or equivalently $\cos\frac{p\pi}{n+1}=0$. The energy dispersion becomes independent of k_x and the eigenenergy always equals $\pm|t|$. A flat band, in general, exists only when n is odd.

(ii) The subbands can be labeled by the quantum number p. Combined with the wave number k_x along the x direction, the quantum number p can be used to define the chirality of the electrons in quasi-one-dimensional (1D) graphene ribbons similar to that in 2D graphene. To identify different subbands, we need the quantum number p_i of the ith conduction or valence band. Here, the definition of the sequence of subbands is referred to as the value of eigenenergy E_C in the center of first Brillouin zone ($k_x=0$),

$$E_C = \pm t\left|2\cos\frac{p\pi}{n+1}+1\right|. \tag{8}$$

For the metallic armchair GNRs with width $n=3m+2$ when $\frac{p\pi}{n+1}=\frac{2\pi}{3}$ or equivalently $p=2m+2$, the energy gap between conduction and valence bands is zero. Therefore p_1 $=2m+2$ corresponds to the first conduction or valence band in $n=3m+2$ GNRs. For the second conduction or valence bands, E_C should have the minimal nonzero value compared to the third or even higher band. After analyzing the value of E_C, we find that $p_2=2m+3$, $p_3=2m+1$ for metallic armchair GNRs ($n=3m+2$). By similar analysis, for $n>10$, we can obtain $p_1=2m+1$, $p_2=2m$, $p_3=2m+2$ for $n=3m$ armchair GNRs and $p_1=2m+1$, $p_2=2m+2$, $p_3=2m$ for $n=3m+1$ armchair GNRs, respectively. For all subbands, there is no general rule of the subband index p.

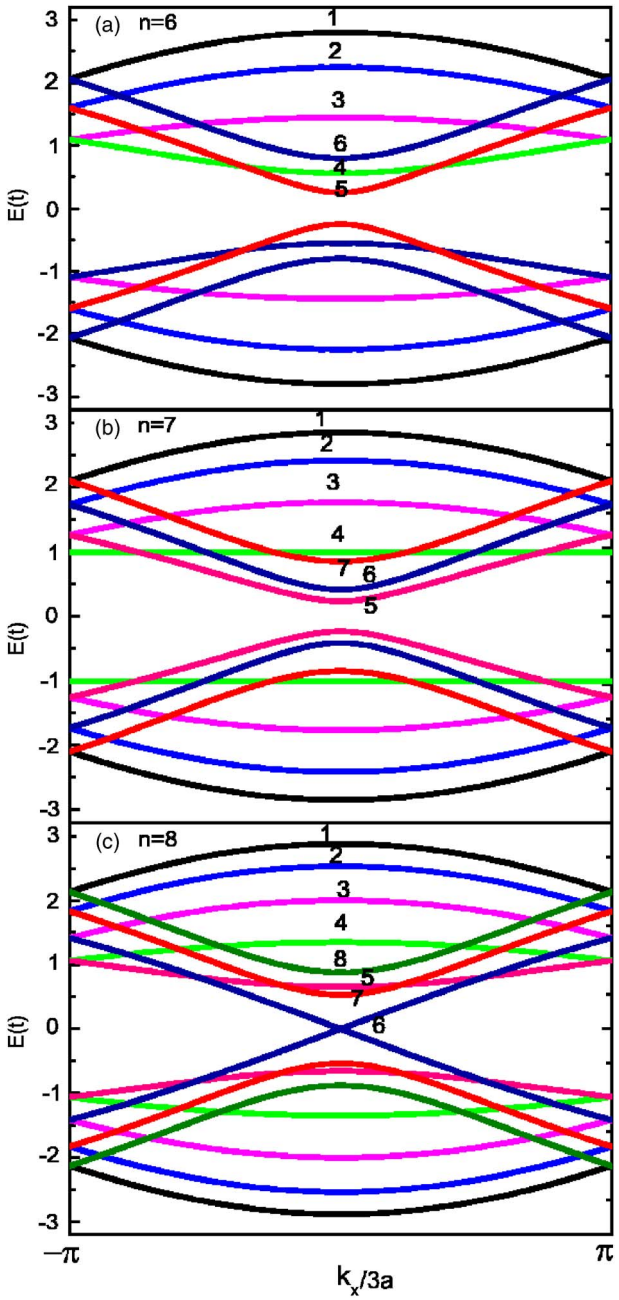

FIG. 2. (Color online) Electronic structures of perfect armchair GNRs with various widths, (a) $n=6$, (b) $n=7$, and (c) $n=8$, respectively. The wave vector is normalized based on the primitive translation vector of individual GNRs. The value of p for each subband is labeled in the figure.

(iii) Lots of research interest have been focusing on the energy dispersion and wave function of 2D graphene and 1D GNRs within the low-energy range.[3,11,14] Low-energy electrons behave as massless relativistic particles in a 2D infinite graphene system.[1–3,6,14] Whether electrons keep their relativistic property when they are confined in quasi-1D graphene nanoribbons is an interesting issue. In what follows, we will focus on the expansion of our analytical expressions to the low-energy limit. When $\frac{p\pi}{n+1} \to \frac{2}{3}\pi$ and $\frac{3k_x a}{2} \to 0$, we rewrite the eigenenergy in Eq. (7) as

$$E \approx \pm \frac{3}{2} at \sqrt{k_x^2 + \tilde{q}_y^2} \approx \pm \hbar v_F k, \tag{9}$$

where $\tilde{q}_y(p) = \frac{2}{\sqrt{3}a}\left(\frac{p\pi}{n+1} - \frac{2}{3}\pi\right)$, p is the subband index. This low-energy expansion generates the $E \propto k$ linear dispersion, with Fermi velocity $v_F \approx 10^6$ m/s. This expression reproduces the result of $\mathbf{k}\cdot\mathbf{p}$ approximation.[14] Note that the wave vector in the confined direction ($\tilde{q}_y$) is discretized, corresponding to different subbands. What is worth mentioning is that this energy dispersion works well only at the low-energy limit. By substituting the value of p_1 into Eq. (9), we get the low-energy expansion of the first conduction or valence band for armchair GNRs as

$$E_1(3m) \overset{k_x \to 0}{\approx} \pm \frac{3}{2} at \sqrt{k_x^2 + \left(\frac{2\pi}{3\sqrt{3}(3m+1)a}\right)^2},$$

$$E_1(3m+1) \overset{k_x \to 0}{\approx} \pm \frac{3}{2} at \sqrt{k_x^2 + \left(\frac{2\pi}{3\sqrt{3}(3m+2)a}\right)^2},$$

$$E_1(3m+2) \overset{k_x \to 0}{\approx} \pm \frac{3at}{2} k_x. \tag{10}$$

Figure 3 shows the quality of low-energy approximation. For large width armchair GNRs, low-energy approximation seems to work well except at the edge of first Brillouin zone. As the width gets larger, the quantum confinement due to the edge becomes less important and the 1D nanoribbons tend to behave like 2D graphene. For large n, as expected, the band structure generates the linear dispersion relationship, $E \propto k$, in the low-energy limit.

In addition, from the expression of the wave function, we also obtain the local density of electronic states in perfect armchair GNRs, $P_A(i) = P_B(i) \propto \sin^2\left(\frac{p\pi}{n+1} i\right)$. Figure 4 shows the squared wave functions of the lowest conduction band at the center of first Brillouin zone. Note that Figs. 4(a) and 4(c) reproduce the results of the $\mathbf{k}\cdot\mathbf{p}$ approximation.[14] The state density oscillates as a function of the lattice position. The oscillation period is related to $\frac{n+1}{p}$. For $n=3m+2$ armchair GNRs, the oscillation period is just 3, which is shown clearly in Fig. 4(a). For $n=3m$, $3m+1$ armchair GNRs, we should write $\frac{n+1}{p}$ into irreducible form $\frac{\alpha}{\beta}$. The oscillation period is then α, which is the numerator of the irreducible form of $\frac{n+1}{p}$. To match the results presented in Ref. 14 we choose $n=51$ and $n=52$ as an example. We get $\alpha=51$ and $\alpha=52$, respectively. As shown in Figs. 4(b) and 4(c), the oscillation period of state density for $n=51$ and $n=52$ armchair GNRs equals their width.

III. ENERGY GAP AND WAVE FUNCTION FOR EDGE-DEFORMED GNR

Because every atom on the edge has one dangling bond unsaturated, the characteristics of the C-C bonds at the edges can change GNRs' electronic structure dramatically.[10,19] To determine the band gaps of GNRs on the scale of nanometer, edge effects should be considered carefully. The change of edge bond length and angle can lead to considerable varia-

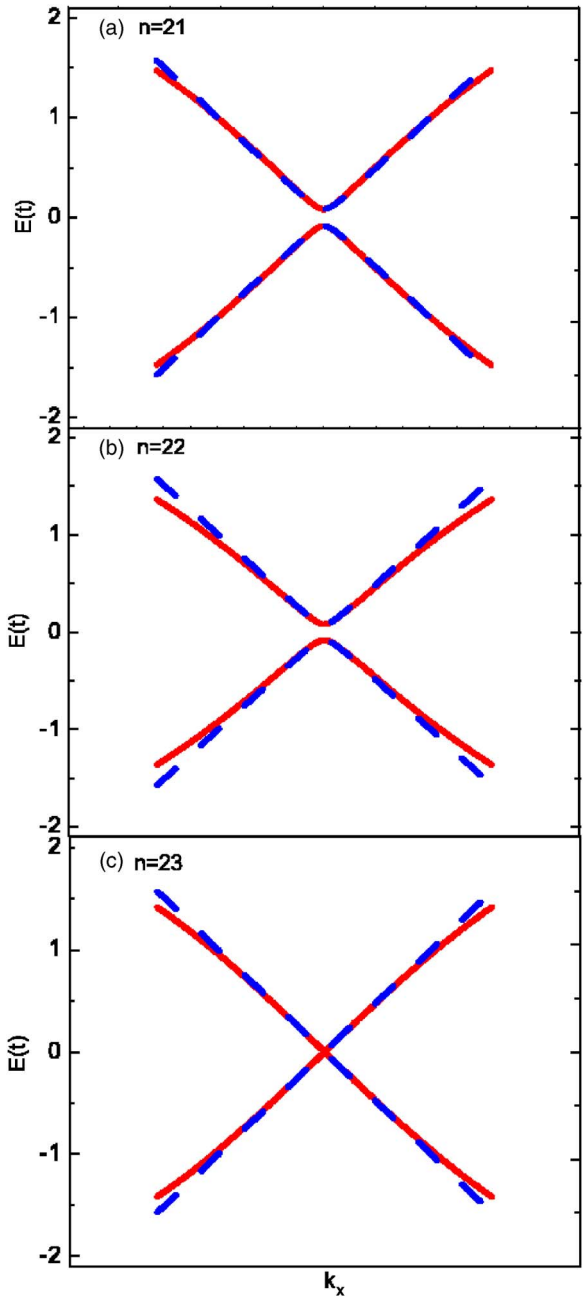

FIG. 3. (Color online) The first conductance and valence bands within the first Brillouin zone: exact solutions from Eq. (7) (red solid line) and low-energy approximation from Eq. (10) (blue dash line) for armchair GNRs with various widths, (a) $n=21$, (b) $n=22$, (c) $n=23$, respectively. The wave vector is normalized based on the primitive translation vector of individual GNRs.

tions of electronic structure, especially within the low-energy range.[11,12] In previously reported work, the edge carbon atoms of GNRs are all passivated by hydrogen atoms or other kinds of atoms or molecules.[10–12,14,19] The bonds between hydrogen and carbon are different from those *C*-*C* bonds. Accordingly, the transfer integral of the *C*-*H* bonds and on-site energy of carbon atoms at the edges are expected to differ from those in the middle of GNRs. The bond lengths between carbon atoms at the edges are predicted to vary

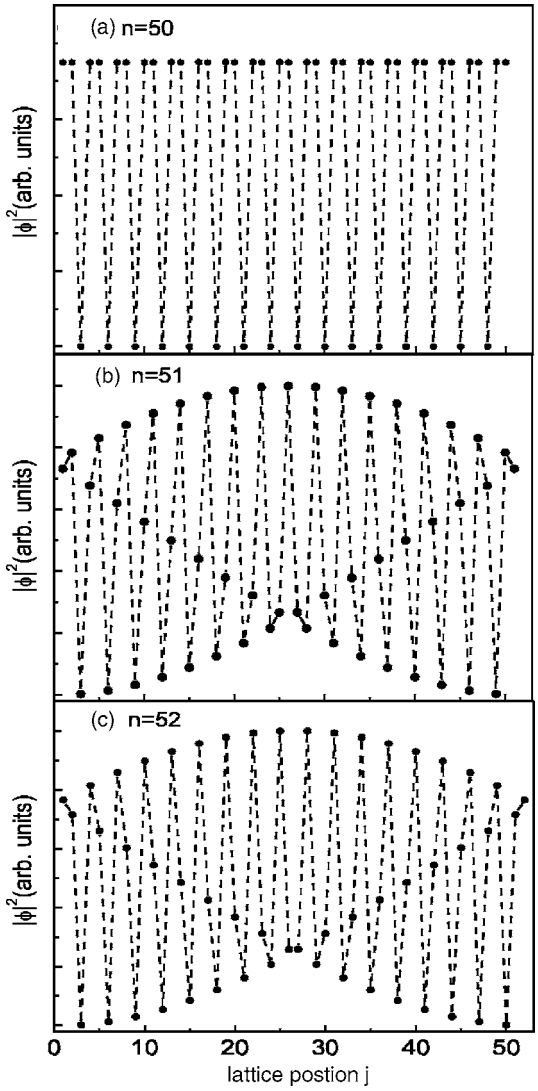

FIG. 4. Local density of the states in the first conduction or valence band at $k_x=0$ for armchair GNRs with various widths, (a) $n=50$, (b) $n=51$, and (c) $n=52$, respectively. (The n is so chosen to match the results in Ref. 14).

about 3–4% when hydrogenerated.[11] Correspondingly, the hopping integral increases about 12% extracted from the analytical tight-binding expression.[18,11] To evaluate the effect of various kinds of edge deformation, we carried out general theoretical calculation and analysis with our analytical solution of armchair GNRs. In general, we can set the variation of the transfer integral and on-site energy as $\delta t_{i,j}$, ε_i for the ith A-type or B-type carbon atom. The Hamiltonian of the GNRs with deformation on the edge can be rewritten as

$$H = \sum_i \varepsilon_i |i\rangle\langle i| - \sum_{\langle i,j\rangle} (t + \delta t_{i,j}) |i\rangle\langle j|. \tag{11}$$

The energy dispersion and wave function are readily obtained by solving the Schrodinger equation with the perturbation approach

$$E = \gamma \pm |\mu + \delta\mu|,$$

$$|\psi\rangle_{\pm} = \frac{\sqrt{2}}{2}\left(|\psi\rangle_A \pm \sqrt{\frac{(\mu+\delta\mu)^*}{\mu+\delta\mu}}|\psi\rangle_B\right), \tag{12}$$

where $\gamma = \frac{2}{n+1}\sum_{i=1}^{n}\varepsilon_i \sin^2\left(\frac{p\pi}{n+1}i\right)$ is the energy shift originating from the variation of on-site energy, while the shift from the hopping integral variation is

$$\delta\mu = -\frac{2}{n+1}\sum_{i=1}^{n}\left[\delta t_{i(A)i(B)} \sin^2\left(\frac{p\pi}{n+1}i\right)e^{-ik_x a} + \delta t_{i(A)i-1(B)} \sin\left(\frac{p\pi}{n+1}i\right)\sin\left(\frac{p\pi}{n+1}(i-1)\right)e^{ik_x a/2} + \delta t_{i(A)i+1(B)} \sin\left(\frac{p\pi}{n+1}i\right)\sin\left(\frac{p\pi}{n+1}(i+1)\right)e^{ik_x a/2}\right]. \tag{13}$$

Such a general expression could include various kinds of small edge deformations, ranging from the quantum confinement effect due to the finite width, to the effect of saturated atoms or molecules attached to edge carbon atoms. This result shows that the deformation leads to a considerable deviation of the energy dispersion relation and wave function of the deformed system from those in perfect armchair GNRs. The local density of states on both kinds of sublattices, however, remains the same as that in perfect armchair GNRs. The reason is that the wave functions of sublattices A and B change their relative phases, but keep the magnitudes unchanged. The variations from both the on-site energy and hopping integral contribute to the energy shift, while the change of on-site energy has no contribution to the wave function as shown in Eq. (12).

To show the impact caused by structural deformation, we model the deformation by using an exponential distribution function as an example. The hopping variations between ith A and ith B atoms are

$$\delta t_{i(A)i(B)} = \delta t_i = \delta t_0 e^{-[L/2-|y(i)|]/\rho_L},$$

$$\delta t_{i(A)i-1(B)} = \delta t_{i(A)i+1(B)} = 0, \tag{14}$$

where $y(i) = \frac{\sqrt{3}}{4}a(2j-n-1)$ is the coordinate of the ith atom in the y direction, $L = \frac{\sqrt{3}}{2}a(n-1)$ is the width of the GNRs. The deformation characteristic length ρ_L is used to indicate the extent of the deformation from the edge to the middle of the GNRs. For example, when $\rho_L \to \infty$, $\delta t_i = \delta_0$ for any i, the deformation is uniform from the edge to the middle; when $\rho_L \to 0$, $\delta t_1 = \delta t_n = \delta t_0$, $\delta t_i = 0$ for $i \neq 1$ or n, the deformation is only localized on the edge bonds.[11] Typically, we set the hopping integral variation $\delta t_0 = 12\% t$ and the hopping integral of perfect GNRs $t = 2.7$ eV.[11] Our perturbation results are valid only when the deformation is small. For example, we have compared the analytical perturbation results with those obtained through numerical diagonalization and found the difference becomes quite large when $\delta t_0 > 15\%$ (the energy gaps obtained from both methods differ by more than 10% when $\delta t_0 > 15\%$). For larger deformation, we should employ the numerical diagolization method or the density-functional theory (DFT) to explore the electronic structure of GNRs.

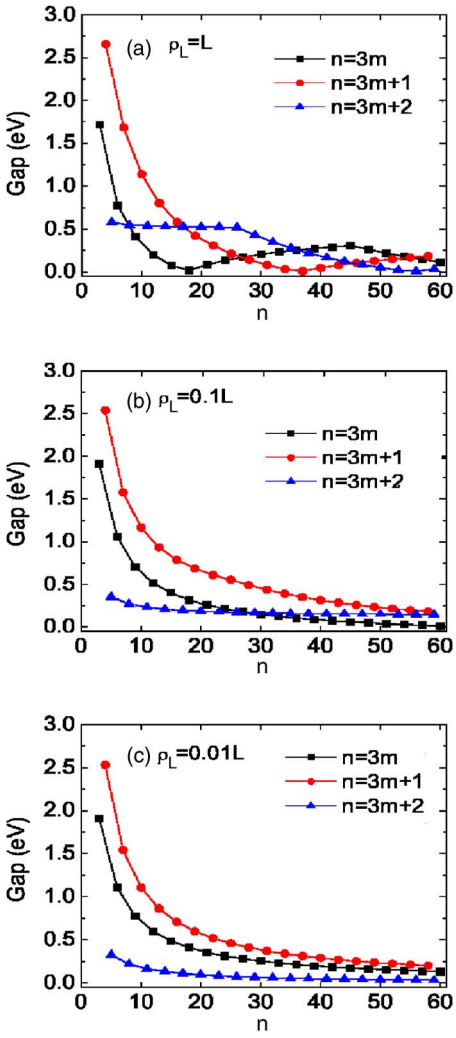

FIG. 5. (Color online) The energy gaps between the lowest conduction band and the highest valence band as a function of width n with the characteristic length (a) $\rho_L = L$, (b) $\rho_L = 0.1L$, and (c) $\rho_L = 0.01L$.

By introducing the deformation, we observe considerable changes of energy gaps compared to those of perfect armchair GNRs. For example, for $n = 6, 7, 8$, the energy gaps are 1.11, 1.54, and 0.22 eV, respectively, when $\rho_L = 0.01L$. They are much larger than those of perfect armchair GNRs (0.49, 0.47, and 0 eV, respectively). All armchair GNRs become semiconducting. The energy gaps between the lowest conduction band and the highest valence band become the function of ribbon width as indicated by three separate curves in Fig. 5. When $\rho_L = L$, the energy gaps fluctuate for large n and three curves cross over. When $\rho_L = 0.1L$, the deformation is localized near the GNR edges and the energy gap for $n = 3m+1$ GNR is always larger than those of $n = 3m$ and $n = 3m+2$ GNRs. When $\rho_L = 0.01L$, the characteristic length is so small that the deformation is localized along two edges, which has been discussed in Ref. 11. The corresponding energy gaps for different width ribbons are as follows:

$$\Delta_{3m} = \Delta_{3m}^0 - \frac{8\delta t}{3m+1}\sin^2\frac{m\pi}{3m+1},$$

$$\Delta_{3m+1} = \Delta_{3m+1}^0 + \frac{8\delta t}{3m+2}\sin^2\frac{(m+1)\pi}{3m+2},$$

$$\Delta_{3m+2} = \Delta_{3m+2}^0 + \frac{2\delta t}{m+1}, \tag{15}$$

where Δ_{3m}^0, Δ_{3m+1}^0, and Δ_{3m+2}^0 are the energy gaps of perfect armchair GNRs. Their values can be extracted from Eq. (8): $2t|2\cos\frac{(2m+1)\pi}{3m+1}+1|$, $2t|2\cos\frac{(2m+1)\pi}{3m+2}+1|$, and 0. This result suggests that all armchair graphene ribbons with edge deformation have nonzero energy gaps and are insulators and $\Delta_{3m+1} > \Delta_{3m} > \Delta_{3m+2}$ for any m.

IV. CONCLUSION

In this paper, we study the electronic states of armchair GNRs analytically. By imposing the hard-wall boundary condition, we find the analytical solution of wave function and energy dispersion in armchair GNRs based on the tight-binding approximation. Our results reproduce the numerical tight-binding calculation results and the solutions using the effective-mass approximation. We also derive the low-energy approximation of the energy dispersion, which matches the exact solution except for the edge of first Brillouin zone. The linear energy dispersion is observed in armchair GNRs in the low-energy limit. In addition, we also evaluate the impact of the edge deformation on GNRs and derive a general expression of wave function and energy dispersion. We can reproduce the energy gap for hydrogenerated armchair GNRs presented in Ref. 11. When we consider the edge deformation, all armchair GNRs have nonzero energy gaps and thus are insulting. Overall, the derived analytical form of the wave function can be used to quantitatively investigate and predict various properties in armchair graphene ribbons.

ACKNOWLEDGMENTS

This work was partially supported by the National Natural Science Foundation of China with Grants No. 10574119, No. 10674121, and No. 50121202. The research was also supported by National Key Basic Research Program under Grant No. 2006CB922000, J. C. would like to acknowledge the funding support from the Discovery program of Natural Sciences and Engineering Research Council of Canada under Grant No. 245680. We also would like to thank Nathanael Wu and Stephen Thornhill for their assistance with the finalization of this paper.

*Corresponding author. Email address: phsqw@ustc.edu.cn
†Corresponding author. Email address: jchen@ece.ualberta.ca

[1] K. S. Novoselov, A. K. Geim, S. V. Morozov, D. Jiang, Y. Zhang, S. V. Dubonos, I. V. Grigorieva, and A. A. Firsov, Science **306**, 666 (2004).
[2] K. S. Novoselov, A. K. Geim, S. V. Morozov, D. Jiang, M. I. Katsnelson, I. V. Grigorieva, S. V. Dubonos, and A. A. Firsov, Nature (London) **438**, 197 (2005).
[3] Yuanbo Zhang, Yan-Wen Tan, Horst L. Stormer, and Philip Kim, Nature (London) **438**, 201 (2005).
[4] Claire Berger, Zhimin Song, Xuebin Li, Xiaosong Wu, Nate Brown, Cécile Naud, Didier Mayou, Tianbo Li, Joanna Hass, Alexei N. Marchenkov, Edward H. Conrad, Phillip N. First, and Walt A. de Heer, Science **312**, 1191 (2006).
[5] Taisuke Ohta, Aaron Bostwick, Thomas Seyller, Karsten Horn, and Eli Rotenberg, Science **313**, 951 (2006).
[6] M. I. Katsnelson, K. S. Novoselov, and A. K. Geim, Nat. Phys. **2**, 620 (2006).
[7] M. Fujita, K. Wakabayashi, K. Nakada, and K. Kusakabe, J. Phys. Soc. Jpn. **65**, 1920 (1996).
[8] K. Nakada, M. Fujita, G. Dresselhaus, and M. S. Dresselhaus, Phys. Rev. B **54**, 17954 (1996).
[9] K. Wakabayashi, M. Fujita, H. Ajiki, and M. Sigrist, Phys. Rev. B **59**, 8271 (1999).
[10] M. Ezawa, Phys. Rev. B **73**, 045432 (2006).
[11] Y.-W. Son, M. L. Cohen, and S. G. Louie, Phys. Rev. Lett. **97**, 216803 (2006).
[12] Y.-W. Son, M. L. Cohen, and S. G. Lioue, Nature (London) **444**, 347 (2006).
[13] Y. Miyamoto, K. Nakada, and M. Fujita, Phys. Rev. B **59**, 9858 (1999).
[14] L. Brey and H. A. Fertig, Phys. Rev. B **73**, 235411 (2006).
[15] C. Berger *et al.*, J. Phys. Chem. B **108**, 19912 (2004).
[16] K. Sasaki, S. Murakami, and R. Saito, J. Phys. Soc. Jpn. **75**, 074713 (2006).
[17] K. Sasaki, S. Murakami, and R. Saito, Appl. Phys. Lett. **88**, 113110 (2006).
[18] D. Porezag, T. Frauenheim, T. Kohler, G. Seifert, and R. Kaschner, Phys. Rev. B **51**, 12947 (1995).
[19] T. Kawai, Y. Miyamoto, O. Sugino, and Y. Koga, Phys. Rev. B **62**, R16349 (2000).
[20] H. Ajiki and T. Ando, J. Phys. Soc. Jpn. **62**, 1255 (1992).